REFERENCES

1. **Akaza I, Yoshimoto T, Tsuchiya K, Hirata Y.** Endothelial dysfunction associated with hypercortisolism is reversible in Cushing's syndrome. *Endocr J* 57: 245–252, 2010.
2. **Barar J, Campbell L, Hollins AJ, Thomas NP, Smith MW, Morris CJ, Gumbleton M.** Cell selective glucocorticoid induction of caveolin-1 and caveolae in differentiating pulmonary alveolar epithelial cell cultures. *Biochem Biophys Res Commun* 359: 360–366, 2007.
3. **Bauer PM, Yu J, Chen Y, Hickey R, Bernatchez PN, Looft-Wilson R, Huang Y, Giordano F, Stan RV, Sessa WC.** Endothelial-specific expression of caveolin-1 impairs microvascular permeability and angiogenesis. *Proc Natl Acad Sci USA* 102: 204–209, 2005.
4. **Baykan M, Erem C, Gedikli O, Hacihasanoglu A, Erdogan T, Kocak M, Durmus I, Korkmaz L, Celik S.** Impairment of flow-mediated vasodilatation of brachial artery in patients with Cushing's syndrome. *Endocrine* 31: 300–304, 2007.
5. **Brostjan C, Anrather J, Csizmadia V, Stroka D, Soares M, Bach FH, Winkler H.** Glucocorticoid-mediated repression of NFkappaB activity in endothelial cells does not involve induction of IkappaBalpha synthesis. *J Biol Chem* 271: 19612–19616, 1996.
6. **Catena C, Colussi G, Nadalini E, Chiuch A, Baroselli S, Lapenna R, Sechi LA.** Cardiovascular outcomes in patients with primary aldosteronism after treatment. *Arch Intern Med* 168: 80–85, 2008.
7. **Cohen AW, Hnasko R, Schubert W, Lisanti MP.** Role of caveolae and caveolins in health and disease. *Physiol Rev* 84: 1341–1379, 2004.
8. **Feron O, Dessy C, Desager JP, Balligand JL.** Hydroxy-methylglutaryl-coenzyme A reductase inhibition promotes endothelial nitric oxide synthase activation through a decrease in caveolin abundance. *Circulation* 103: 113–118, 2001.
9. **Galbiati F, Volonte D, Engelman JA, Watanabe G, Burk R, Pestell RG, Lisanti MP.** Targeted downregulation of caveolin-1 is sufficient to drive cell transformation and hyperactivate the p42/44 MAP kinase cascade. *EMBO J* 17: 6633–6648, 1998.
10. **Gill GN, Ill CR, Simonian MH.** Angiotensin stimulation of bovine adrenocortical cell growth. *Proc Natl Acad Sci USA* 74: 5569–5573, 1977.
11. **Gonzalez E, Kou R, Michel T.** Rac1 modulates sphingosine 1-phosphate-mediated activation of phosphoinositide 3-kinase/Akt signaling pathways in vascular endothelial cells. *J Biol Chem* 281: 3210–3216, 2006.
12. **Gonzalez E, Nagiel A, Lin AJ, Golan DE, Michel T.** Small interfering RNA-mediated down-regulation of caveolin-1 differentially modulates signaling pathways in endothelial cells. *J Biol Chem* 279: 40659–40669, 2004.
13. **Greenberger S, Boscolo E, Adini I, Mulliken JB, Bischoff J.** Corticosteroid suppression of VEGF-A in infantile hemangioma-derived stem cells. *N Engl J Med* 362: 1005–1013, 2010.
14. **Igarashi J, Miyoshi M, Hashimoto T, Kubota Y, Kosaka H.** Statins induce S1P(1) receptors and enhance endothelial nitric oxide production in response to high-density lipoproteins. *Br J Pharmacol* 150: 470–479, 2007.
15. **Igarashi J, Shoji K, Hashimoto T, Moriue T, Yoneda K, Takamura T, Yamashita T, Kubota Y, Kosaka H.** Transforming growth factor-beta1 downregulates caveolin-1 expression and enhances sphingosine 1-phosphate signaling in cultured vascular endothelial cells. *Am J Physiol Cell Physiol* 297: C1263–C1274, 2009.
16. **Kasselman LJ, Kintner J, Sideris A, Pasnikowski E, Krellman JW, Shah S, Rudge JS, Yancopoulos GD, Wiegand SJ, Croll SD.** Dexamethasone treatment and ICAM-1 deficiency impair VEGF-induced angiogenesis in adult brain. *J Vasc Res* 44: 283–291, 2007.
17. **Kim KH, Moriarty K, Bender JR.** Vascular cell signaling by membrane estrogen receptors. *Steroids* 73: 864–869, 2008.
18. **Kristo C, Ueland T, Godang K, Aukrust P, Bollerslev J.** Biochemical markers for cardiovascular risk following treatment in endogenous Cushing's syndrome. *J Endocrinol Invest* 31: 400–405, 2008.
19. **Labrecque L, Royal I, Surprenant DS, Patterson C, Gingras D, Beliveau R.** Regulation of vascular endothelial growth factor receptor-2 activity by caveolin-1 and plasma membrane cholesterol. *Mol Biol Cell* 14: 334–347, 2003.
20. **Leopold JA, Dam A, Maron BA, Scribner AW, Liao R, Handy DE, Stanton RC, Pitt B, Loscalzo J.** Aldosterone impairs vascular reactivity by decreasing glucose-6-phosphate dehydrogenase activity. *Nat Med* 13: 189–197, 2007.
21. **Levine YC, Li GK, Michel T.** Agonist-modulated regulation of AMP-activated protein kinase (AMPK) in endothelial cells: evidence for an AMPK -> Rac1 -> Akt -> endothelial nitric-oxide synthase pathway. *J Biol Chem* 282: 20351–20364, 2007.
22. **Li L, Yang G, Ebara S, Satoh T, Nasu Y, Timme TL, Ren C, Wang J, Tahir SA, Thompson TC.** Caveolin-1 mediates testosterone-stimulated survival/clonal growth and promotes metastatic activities in prostate cancer cells. *Cancer Res* 61: 4386–4392, 2001.
23. **Liu J, Razani B, Tang S, Terman BI, Ware JA, Lisanti MP.** Angiogenesis activators and inhibitors differentially regulate caveolin-1 expression and caveolae formation in vascular endothelial cells. Angiogenesis inhibitors block vascular endothelial growth factor-induced down-regulation of caveolin-1. *J Biol Chem* 274: 15781–15785, 1999.
24. **Liu P, Li WP, Machleidt T, Anderson RG.** Identification of caveolin-1 in lipoprotein particles secreted by exocrine cells. *Nat Cell Biol* 1: 369–375, 1999.
25. **Luo JC, Shin VY, Liu ES, Ye YN, Wu WK, So WH, Chang FY, Cho CH.** Dexamethasone delays ulcer healing by inhibition of angiogenesis in rat stomachs. *Eur J Pharmacol* 485: 275–281, 2004.
26. **Mancini T, Kola B, Mantero F, Boscaro M, Arnaldi G.** High cardiovascular risk in patients with Cushing's syndrome according to 1999 WHO/ISH guidelines. *Clin Endocrinol (Oxf)* 61: 768–777, 2004.
27. **Michel T, Feron O.** Nitric oxide synthases: which, where, how, and why? *J Clin Invest* 100: 2146–2152, 1997.
28. **Nagata D, Takahashi M, Sawai K, Tagami T, Usui T, Shimatsu A, Hirata Y, Naruse M.** Molecular mechanism of the inhibitory effect of aldosterone on endothelial NO synthase activity. *Hypertension* 48: 165–171, 2006.
29. **Neufeld G, Cohen T, Gengrinovitch S, Poltorak Z.** Vascular endothelial growth factor (VEGF) and its receptors. *FASEB J* 13: 9–22, 1999.
30. **Patel HH, Murray F, Insel PA.** Caveolae as organizers of pharmacologically relevant signal transduction molecules. *Annu Rev Pharmacol Toxicol* 48: 359–391, 2008.
31. **Salatino M, Beguelin W, Peters MG, Carnevale R, Proietti CJ, Galigniana MD, Vedoy CG, Schillaci R, Charreau EH, Sogayar MC, Elizalde PV.** Progestin-induced caveolin-1 expression mediates breast cancer cell proliferation. *Oncogene* 25: 7723–7739, 2006.
32. **Scherer PE, Lisanti MP, Baldini G, Sargiacomo M, Mastick CC, Lodish HF.** Induction of caveolin during adipogenesis and association of GLUT4 with caveolin-rich vesicles. *J Cell Biol* 127: 1233–1243, 1994.
33. **Song KS, Li S, Okamoto T, Quilliam LA, Sargiacomo M, Lisanti MP.** Co-purification and direct interaction of Ras with caveolin, an integral membrane protein of caveolae microdomains. Detergent-free purification of caveolae microdomains. *J Biol Chem* 271: 9690–9697, 1996.
34. **Sonveaux P, Martinive P, DeWever J, Batova Z, Daneau G, Pelat M, Ghisdal P, Gregoire V, Dessy C, Balligand JL, Feron O.** Caveolin-1 expression is critical for vascular endothelial growth factor-induced ischemic hindlimb collateralization and nitric oxide-mediated angiogenesis. *Circ Res* 95: 154–161, 2004.
35. **Tauchmanova L, Rossi R, Biondi B, Pulcrano M, Nuzzo V, Palmieri EA, Fazio S, Lombardi G.** Patients with subclinical Cushing's syndrome due to adrenal adenoma have increased cardiovascular risk. *J Clin Endocrinol Metab* 87: 4872–4878, 2002.
36. **Tsukamoto I, Sakakibara N, Maruyama T, Igarashi J, Kosaka H, Kubota Y, Tokuda M, Ashino H, Hattori K, Tanaka S, Kawata M, Konishi R.** A novel nucleic acid analogue shows strong angiogenic activity. *Biochem Biophys Res Commun* 399: 699–704, 2010.
37. **van Batenburg MF, Li H, Polman JA, Lachize S, Datson NA, Bussemaker HJ, Meijer OC.** Paired hormone response elements predict caveolin-1 as a glucocorticoid target gene. *PLos One* 5: e8839, 2010.
38. **Wallerath T, Godecke A, Molojavyi A, Li H, Schrader J, Forstermann U.** Dexamethasone lacks effect on blood pressure in mice with a disrupted endothelial NO synthase gene. *Nitric Oxide* 10: 36–41, 2004.
39. **Wallerath T, Witte K, Schafer SC, Schwarz PM, Prellwitz W, Wohlfart P, Kleinert H, Lehr HA, Lemmer B, Forstermann U.** Down-regulation of the expression of endothelial NO synthase is likely to contribute to glucocorticoid-mediated hypertension. *Proc Natl Acad Sci USA* 96: 13357–13362, 1999.
40. **Walters EH, Reid D, Soltani A, Ward C.** Angiogenesis: a potentially critical part of remodelling in chronic airway diseases? *Pharmacol Ther* 118: 128–137, 2008.
41. **Yoneda K, Fujimoto T, Imamura S, Ogawa K.** Distribution of fodrin in the keratinocyte in vivo and in vitro. *J Invest Dermatol* 94: 724–729, 1990.

Experimental dermatology • **Original article**

CED
Clinical and Experimental Dermatology

Sphingosine 1-phosphate attenuates peroxide-induced apoptosis in HaCaT cells cultured *in vitro*

T. Moriue,[1] J. Igarashi,[2] K. Yoneda,[1] T. Hashimoto,[2] K. Nakai,[2] H. Kosaka[2] and Y. Kubota[1]

Departments of [1]Dermatology and [2]Cardiovascular Physiology, Faculty of Medicine, Kagawa University, Kagawa, Japan

doi:10.1111/ced.12037

Summary

Background. Sphingosine 1-phosphate (S1P) is a sphingolipid mediator that elicits a wide array of physiological responses in various types of mammalian cells. Among the numerous biological activities elicited by S1P is protection from apoptotic cell death, which seems to take place through the cell-surface S1P receptor and the downstream phosphoinositide 3′-OH kinase (PI3-K)/Akt pathway. It is unclear whether and how S1P protects human keratinocytes from hydrogen peroxide (H_2O_2)-induced apoptosis.

Aim. We investigated the effects of S1P on apoptotic cell death in HaCaT cells, spontaneously immortalized human keratinocytes.

Methods. HaCaT cells were treated with hydrogen peroxide (H_2O_2) 1–2 mmol/L as an inducer of apoptosis. Cellular apoptosis was assessed with terminal dUTP nick-end labelling (TUNEL), WST-8 and immunoblot assays.

Results. In WST-8 and TUNEL assays, S1P pretreatment (1 μmol/L for 30 min) attenuated H_2O_2-induced cell death. Promotion of the cleavage of caspase-3 by H_2O_2 was markedly attenuated when cells had been preincubated with S1P. S1P markedly potentiated phosphorylation (activation) of Akt in the presence of H_2O_2. Wortmannin, a selective inhibitor of the PI3-K/Akt pathway, significantly suppressed S1P-induced attenuation of caspase-3 cleavage promoted by H_2O_2.

Conclusions. S1P, a sphingolipid mediator, attenuates H_2O_2-induced apoptosis of HaCaT cells, by promoting phosphorylation of the Akt pathway.

Introduction

Sphingosine 1-phosphate (S1P) is a sphingolipid mediator that elicits a wide variety of biological actions in numerous mammalian cell types.[1] Specifically in keratinocytes, S1P evokes such important responses as proliferation,[2] differentiation[2,3] and migration.[4] An antiapoptotic effect represents another important function of S1P. In keratinocytes, S1P attenuates apoptotic cell death induced by actinomycin, tumour necrosis factor (TNF)-α,[5] ceramide[6] and ultraviolet (UV)B irradiation.[7]

It is known that skin wounding causes oxidative stress, defined as excess production of reactive oxygen species (ROS). For example, increased levels of hydrogen peroxide (H_2O_2) are detected in wound fluid.[8] Oxidative stress may function as a 'double-edged sword' in the wound-healing process, as it promotes coagulation, initiation of inflammation, re-epithelization, angiogenesis and matrix deposition, while inhibiting migration and inducing apoptosis in keratinocytes.[9] It is therefore important to better elucidate the effects of ROS on keratinocytes and how bioactive substances modulate such processes.

Recently, we reported that S1P attenuates H_2O_2-induced apoptosis of cultured vascular endothelial cells, associated with attenuation of p38 MAP kinase

Correspondence: Dr Tetsuya Moriue, Department of Dermatology, Faculty of Medicine, Kagawa University, 1750-1 Ikenobe, Miki-Cho, Kita-Gun, Kagawa 761-0793, Japan
E-mail: moririn@med.kagawa-u.ac.jp

Conflict of interest: none declared.

Accepted for publication 22 July 2012

activation.[10] However, it remains unclear whether and how S1P protects human keratinocytes from H_2O_2-induced apoptosis.[11] In the present study, we investigated the effects of S1P on apoptotic cell death in HaCaT cells, spontaneously immortalized human keratinocytes.

Methods

Cell culture and drug treatments

HaCaT cells[12,13] were split at a ratio of 1 : 4 and maintained in DMEM (Sigma Chemical Co., St. Louis, MO, USA), supplemented with heat-inactivated fetal bovine serum (FBS; 10%, v/v) and streptomycin (100 U/mL and 100 mg/mL) on culture plates. They were kept at 37 °C in a humidified atmosphere containing 5% CO_2. At 70–80% confluence, the culture medium was changed to DMEM without FBS, and the cells incubated for 30 min before any further experiments to exclude the effects of any residual S1P contained in the FBS.

WST-8 assay of cell viability

HaCaT cell viability was assessed using a 2-(2-methoxy-4-nitrophenyl)-3-(4-nitrophenyl)-5-(2,4-disulfophenyl)-2H-tetrazolium (WST-8) assay, in accordance with the manufacturer's instructions. Briefly, cells were split at a ratio of 1 : 8 and were transferred to a 96-well plate, then mixed with 10 μl of CCK-8 solution from a commercial kit (Dojindo, Tokyo, Japan).and incubated for 1 h at 37 °C in a CO_2 incubator. Some cells were pretreated with 1 μmol/L S1P for 30 min, and all cells (pretreated or not) were then treated with 750 μmol/L H_2O_2 or vehicle for 4 h. After treatment, cells were mixed with 10 μL of CCK-8 solution from a commercial kit (Dojindo, Tokyo, Japan), and incubated for 1 h at 37 °C in a CO_2 incubator. Cell viability was determined by measuring optical density (OD) at 450 nm using a microplate reader (model SH-9000; Hitachi Hi-Technologies, Tokyo, Japan) In each experiment, the OD 450 nm values were normalized to those with H_2O_2 alone, which yielded minimum values within each experiment.

Terminal dUTP nick-end labelling assay

The degrees of DNA nick formation were determined *in situ* by a terminal dUTP nick-end labelling (TUNEL) assay. HaCaT cells were split at a ratio of 1 : 24 and seeded onto coverslips. At approximately 30% confluence, 4 days after being split, the cells were starved of serum. They were washed with phosphate-buffered saline (PBS) on ice, and fixed with 1% paraformaldehyde in PBS (w/v) for 10 min at ambient temperature, followed by permeabilization with acetone/ethanol (1 : 2 v/v) for 5 min at −20 °C. The TUNEL assay was then performed with a commercial kit (ApopTag Fluorescein *In Situ* Apoptosis Detection Kit; Chemicon, Temecula, CA, USA) in accordance with the the manufacturer's instructions. To determine the number of TUNEL-positive cells, 1000 cells were counted using fluorescent microscopy, with five independent microscopic fields counted in each coverslip at ×40 magnification. The percentage of TUNEL-positive cells was calculated as:

(total number of TUNEL-positive cells ÷ total number of all cells) × 100.

Immunoblotting analyses

HaCaT cells were split at a ratio of 1 : 4, and cultured on plastic dishes. Immunoblotting analyses were performed as described previously.[14] Briefly, the membrane was probed with an antibody against the cleaved form of caspase-3 (Asp^{175}) protein (Cell Signaling Technology Inc., Beverly, MA, USA). Equal amounts of protein (50 μg) were loaded per lane. Blots were re-probed with an antibody directed to (total) actin to confirm equal loading (not shown). Signals corresponding to the cleaved form of caspase-3 were quantified and normalized against the value obtained with H_2O_2 alone (maximum) in each experiment.

Akt analyses

HaCaT cells were divided into two groups: one group was pretreated with S1P 1 μmol/L for 30 min, then all cells were treated with H_2O_2 1 mmol/L for 0, 5, 15, 30, 45 and 60 minutes. Signals corresponding to phosphorylated forms of Akt were quantified and normalized against the values obtained using antibodies specific to total Akt (Cell Signaling Technology Inc.). Equal amounts of protein (30 μg) were loaded per lane, and the resulting ratios of phosphorylated (Ser^{473}; Cell Signaling Technology Inc.) to total Akt were then normalized to the basal value obtained in the absence of H_2O_2 and S1P.

Cells were also treated with wortmannin (Merck, Darmstadt, Germany) dissolved in 0.1% (v/v) dimethyl sulfoxide (DMSO) to examine the effect on H_2O_2-induced phosphorylation of Akt and cleavage of caspase-3. HaCaT cells were pretreated with wortmannin 10 nmol/L for 30 min, then treated with $H2O_2$ or

vehicle (distilled water) for 15 min. Equal amounts of protein (100 μg) were loaded onto protein gels and immunoblotted. Some cells were pretreated with S1P 1 μmol/L for 30 min, and the membrane was probed for the cleaved form of caspase-3 protein. Equal amounts of protein (100 μg) were loaded per lane, and blots were re-probed with an antibody directed to total actin to confirm equal loading.

Supplementary experiments

We used reverse transcription (RT)-PCR to detect transcripts encoding $S1P_1$ to $S1P_5$ (see supplementary figures for details). Actin and glyceraldehyde 3-phosphate dehydrogenase were used as housekeeping genes (Table S1).

Next, HaCaT cells were pretreated with FTY720-P1 (Cayman Chemical Co., Ann Arbor, MI, USA) 1 μmol/L for 30 min to assesses whether it enhanced H_2O_2-elicited Akt phosphorylation.

Activation of signal transducer and activator of transcription (Stat)3, which mediates the H_2O_2-elicited cellular damage, was also assessed, using phospho-Stat3 (Tyr^{705}/Ser^{727}; Cell Signaling Technology Inc.).

We also evaluated the effects of H_2O_2 and/or S1P on mitogen-activated protein kinases (MAPKs) by assessing the degrees of phosphorylation, using antibodies to phospho-p38 (Thr^{180}/Tyr^{182}), total p38, phospho-Jun kinase (JNK; Thr^{183}/Tyr^{185}), total JNK, phospho-extracellular signal-regulated kinase (ERK)1/2 (Thr^{202}/Tyr^{204}) and total ERK1/2 (all Cell Signaling Technology Inc.).

Statistical analysis

All experiments were performed at least 3 times. Mean values for individual experiments are expressed as means ± SE. Significant differences between two groups were analysed by Student's *t*-test using Microsoft Excel. $P < 0.05$ was considered significant.

Results

WST-8 assay of cell viability

The WST-8 assay showed that survival of HaCaT cells 4 h after treatment with H_2O_2 750 μmol/L was significantly ($P = 0.04$) decreased to 57.9 ± 7.4% of baseline (Fig. 1a). Importantly, when cells had been exposed to S1P before H_2O_2, attenuation of cellular viability was reversed to 82.5 ± 6.2% ($P = 0.04$).

Terminal dUTP nick-end labelling assay

A significantly larger number of TUNEL-positive nuclei (Fig. 1: green staining, arrowheads) were seen in HaCaT cells 4 h after treatment with H_2O_2 750 μmol/L compared with untreated cells, showing that their DNA was nicked upon H_2O_2 treatment. The fraction of TUNEL-positive cells increased after H_2O_2 treatment by 14-fold from basal levels ($P = 0.01$). Pretreatment with 1 μmol/L S1P decreased the fraction of TUNEL-positive cells by 21.4% ($P = 0.03$) compared with those treated with H_2O_2 alone (Fig. 1c).

Immunoblotting analyses

H_2O_2 induced cleavage (activation) of caspase-3 protein, which was markedly attenuated when cells were preincubated with S1P.

Akt analyses

The amount of phosphorylated Akt, increased slightly, but did not reach significance after treatment with H_2O_2 750 μmol/L alone (Fig. 2). However, pretreatment with S1P 1 μmol/L for 30 min significantly enhanced the H_2O_2-elicited Akt phosphorylation, and this was visible 15 min after H_2O_2 treatment.

Pretreatment with wortmannin significantly ($P = 0.001$) attenuated the degree of S1P-induced phosphorylation of Akt (Fig. 3a), and markedly increased H_2O_2-evoked cleavage of caspase-3 ($P < 0.01$). S1P was incapable of protecting HaCaT cells from the H_2O_2-elicited cleavage of caspase-3 in the presence of wortmannin (Fig. 3b).

Supplementary experiments

Using RT-PCR, transcripts encoding $S1P_1$ to $S1P_5$ were detected (Fig. S1).

Pretreatment of HaCaT cells with FTY720-P 1 μmol/L for 30 min significantly enhanced the H_2O_2-elicited Akt phosphorylation at 5 min (Fig. S2).

We explored Stat3 phosphorylation with western blot analysis. When cells were pretreated with FTY720-P, phosphorylation of Ser^{727} was attenuated ($P < 0.05$) but not that of $Tyr7^{05}$ (Fig. S3).

H_2O_2 induced a robust phosphorylation (activation) response of MAPKs. S1P did not affect the degree of phosphorylation of p38, JNK and ERK1/2 (data not shown). An increase in S1P from 1 to 10 μmol/L did not alter the degree of Akt phosphorylation in the presence of successively administered H_2O_2 (Fig S4),

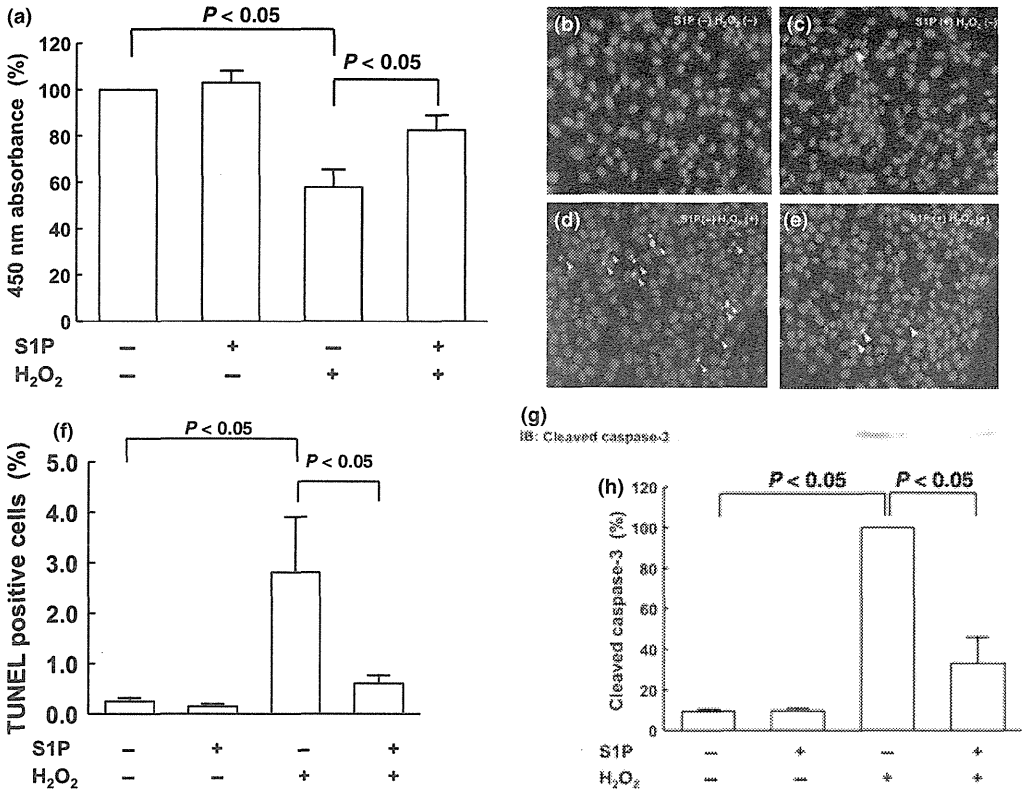

Figure 1 (a) In the WST-8 assay, sphingosine 1-phosphate (S1P) pretreatment reduced the H_2O_2-induced apoptotic responses of HaCaT cells. Each data point represents mean ± SE; $n = 4$. (b–e) Terminal dUTP nick-end labelling assay, using fluorescent microscopy (yellow arrowheads indicate TUNEL-positive signals). (f) Quantification of TUNEL-positive cell numbers as a percentage of the total. Each data point represents mean ± SE; $n = 5$. (g) Representative image of immunoblot after H_2O_2/S1P treatment. The membrane was probed for the cleaved form of caspase-3 protein, and re-probed with an antibody directed to (total) actin to confirm equal loading (not shown). (h) Densitometric analyses: signals corresponding to cleaved caspase-3 were quantified and normalized against H_2O_2 alone (maximum). Each data point represents mean ± SE; $n = 3$.

but did attenuate the H_2O_2-induced cleavage of caspase-3 in HaCaT cells (Fig. S5), as we saw when we re-probed the left four lanes separately.

Discussion

We examined the effect of H_2O_2 and S1P in HaCaT cells. We found that S1P attenuated the H_2O_2-induced apoptosis in HaCaT cells, as assessed by the WST assay. Using TUNEL, it was found that H_2O_2 induced DNA fragmentation in HaCaT cells, and again, this was reduced by treatment with S1P. Our findings that S1P is able to counteract H_2O_2-dependent apoptotic responses of HaCaT cells are consistent with earlier reports suggesting that S1P could be a pro-survival sphingolipid metabolite. For example, S1P keeps keratinocyte cultures from undergoing apoptosis elicited by stimuli such as TNF-α[5] and UVB.[7] These earlier studies primarily focused on the roles of endogenous S1P. To our knowledge, the present report is the first to show antiapoptotic effects of exogenous S1P in HaCaT cells.

Caspase-3 is a key 'executor' protease of apoptotic processes of HaCaT cells.[15] We therefore examined the effects of H_2O_2 and/or S1P on caspase-3 by performing immunoblot analyses of HaCaT cells, using an antibody specific to the cleaved (activated) form of caspase-3. The H_2O_2-induced cleavage of caspase-3 protein was markedly reduced by preincubation with S1P.

The protein kinase Akt is a well-established antiapoptotic protein. It is one of the downstream effector proteins of the S1P receptor pathway, and stimulation of S1P receptors in keratinocytes leads to Akt activation.[11] Inhibitors ofAkt attenuate the antiapoptotic effects of Akt in keratinocytes.[16] Therefore, we evaluated the effects of H_2O_2 and/or S1P on Akt by assessing

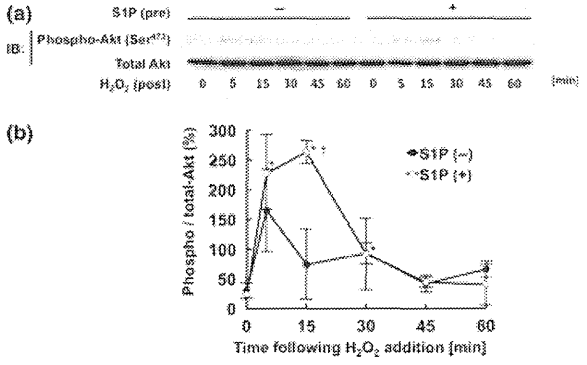

Figure 2 (a,b) Sphingosine 1-phosphate (S1P) pretreatment enhances H_2O_2-induced phosphorylation of Akt in HaCaT cells. HaCaT cells were pre-treated or not with S1P 1 μmol/L for 30 min, then treated with H_2O_2 1 mmol/L for the indicated times. (a) Equal amounts of protein (30 μg) were loaded per lane. (b) The resulting ratios of phospho-Akt to total Akt were then normalized to the basal value obtained in the absence of H_2O_2 and S1P. Each data point represents mean ± SE. Open and closed circles represent values obtained with and without pretreatment with S1P, respectively. *$P < 0.05$ vs. 0 min, †$P < 0.05$ vs. S1P (–); $n = 7$.

the degrees of phosphorylation. The ratio of phosphorylated Akt at serine 473 was determined by using antibodies that recognize Akt and comparing the relative densitometry on immunoblots of activated Akt with the adjusted values of total Akt protein. Akt did not increase significantly with H_2O_2 alone, but did increase after pretreatment with S1P. Thus we sought to explore the roles of S1P receptors in our system.

We used a pharmacological inhibitor of PI3-K, wortmannin, to assess the effects of PI3-K inhibition. Pretreatment with this agent reduced S1P-induced phosphorylation of Akt and increased H_2O_2-evoked cleavage of caspase-3. In the presence of wortmannin, S1P was unable to prevent H_2O_2-elicited cleavage of caspase-3. These results indicate that the protective effects of S1P against H_2O_2-elicited apoptotic responses in HaCaT cells were mediated by the PI3-K/Akt pathway.

To explore the roles of S1P receptors in our system, we used RT-PCR in HaCaT cells, and detected transcripts encoding encoding $S1P_1$– $S1P_5$.

Recently, the therapeutic effects of S1P and S1P receptor-related agents have been assessed for certain condiions. For example, FTY720, which acts as an S1P receptor agonist when phosphorylated, has been used for the treatment of multiple sclerosis.[17] FTY720 also improved the degrees of contact hypersensitivity in a mouse model.[18] We investigated whether FTY720-P promotes H_2O_2-induced Akt phosphorylation. H_2O_2-elicited Akt phosphorylation was significantly enhanced when HaCaT cells were pretreated with FTY720-P, supporting the hypothesis that S1P attenuates H_2O_2-induced apoptosis as an S1P receptor agonist rather than as an intracellular second messenger.

We also assessed the effect of FTY720-P on Stat3, which is a mediator of H_2O_2-elicited cellular damage in normal human keratinocytes.[19] When HaCaT cells were pretreated with FTY720-P, the degree of serine 727 phosphorylation was reduced, but not that of tyrosine 705. Thus, Stat3 represents another potential

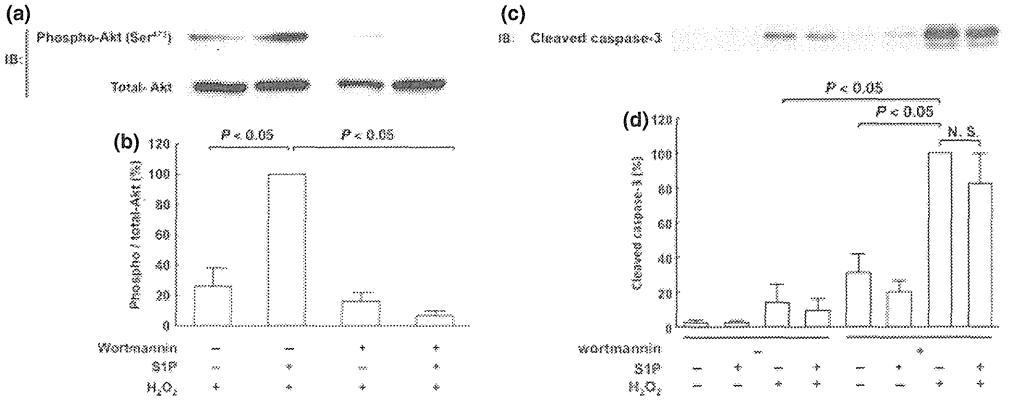

Figure 3 Wortmannin attenuates H_2O_2-induced phosphorylation of Akt and cleavage of caspase-3. (a,b) HaCaT cells were pretreated with wortmannin 10 nmol/L for 30 min, then treated with $H2O_2$ or vehicle (distilled water) for 15 min. (a) Equal amounts of protein (100 μg) were loaded per lane, and (b) analysed densitometrically. Data are expressed as means ± SE, $n = 3$. (c) HaCaT cells were pretreated with wortmannin 10 nmol/L for 30 min, then treated with S1P 1 μmol/L for 30 min, and the resulting membrane was probed for the cleaved form of caspase-3. (c) Equal amounts of protein (100 μg) were loaded per lane, and (d) analysed densitometrically. Data are expressed as means ± SE, $n = 4$. IB, immunoblot.

target of the S1P receptor system in H_2O_2-exposed HaCaT cells.

A wide array of other signalling proteins have been suggested as proximal molecules that connect cellular stimulation with execution of apoptosis. The MAPKs p38 and JNK have been previously implicated in oxidative stress-induced apoptosis in keratinocytes,[20] and we previously found that S1P protects cultured vascular endothelial cells from H_2O_2-induced apoptosis, associated with attenuation of p38 MAPK activation.[10] We therefore sought to explore whether S1P attenuates H_2O_2-induced apoptosis by modulating the activity of these molecules. We found that the MAPKs underwent robust phosphorylation (activation) responses. S1P did not affect the degree of phosphorylation of p38, JNK or ERK1/2 (data not shown). These results indicate that the PI3-K/Akt pathway may be more important than MAPKs in the anti-apoptotic effect of S1P in HaCaT cells.

In a previous study on vascular endothelial cells, H_2O_2 was shown to promote phosphorylation of Akt,[21] but in our study, we found that H_2O_2 by itself did not enhance phosphorylation of Akt in HaCaT cells. Schuppel *et al.* reported that high-dose (10 μmol/L) S1P attenuated phosphorylation of Akt in normal human keratinocytes[11]; however, we found that an increase of S1P from 1 to 10 μmol/L did not alter the degree of Akt phosphorylation in the presence of successively administered H_2O_2. The reason for this discrepancy is unknown. It may be due to the difference between HaCaT cells and primary keratinocytes. Nevertheless, our study suggests that a physiologically relevant concentration of S1P, i.e. 1 μmol/L, rather than pharmacological concentrations, seems to enhance phosphorylation of Akt. However, we used the concentration of 1 μmol/L because serum S1P concentrations seem to be within the range of several hundred nanomoles to a few micromoles in most (patho-)physiological conditions.[22] Our findings that the antiapoptotic effects of S1P act via phosphorylation of Akt are consistent with earlier reports showing that the PI3-K/Akt pathway is a major target of S1P in various cell types, including vascular endothelial cells.[23]

In our study, exogenously added S1P attenuated H_2O_2-elicited apoptotic responses in HaCaT cells, indicating the S1P receptors and the PI3K/Akt pathway as potential molecular targets of S1P-induced anti-apoptotic actions in these conditions. FTY720-P can also modulate cellular function by an S1P receptor-independent pathway.[24] Thus, although S1P receptor activation probably drives the PI3-K/Akt pathway, our results do not completely exclude the possibility that some of the effects of S1P are mediated in a receptor-independent fashion.

We propose that the antiapoptotic effects of S1P have potential clinical relevance, because H_2O_2 is derived from wound fluid,[8] and oxidative stress has a negative effect on wound healing via apoptosis of keratinocytes and vascular endothelial cells.[9] In an earlier study, we found that S1P attenuated oxidative stress-induced apoptosis in cultured endothelial cells.[10] The recent study by Kawanabe *et al.* provided the intriguing observation that addition of a high concentration of S1P had a therapeutic effect on wounded skin in diabetic, but not normal, mice.[25] Because our experiments were performed in HaCaT cells derived from humans, our data imply that S1P could also contribute to promotion of wound healing in humans.

Conclusion

S1P, a sphingolipid mediator, attenuates H_2O_2-induced apoptosis of HaCaT cells, via phosphorylation of Akt. S1P may have clinical relevance in a number of clinical conditions. Further investigations need to be performed to explore these interesting possibilities.

What's already known about this topic?

- In earlier studies, S1P was shown to prevent keratinocyte cultures from undergoing apoptosis elicited by stimuli such as TNF-α and UVB irradiation.
- These studies primarily focused on the roles of endogenous S1P.

What does this study add?

- To our knowledge, this is the first report of the anti-apoptotic effects of exogenous S1P in HaCaT cells.
- Our results demonstrate that the protective effects of S1P against H_2O_2-elicited apoptotic responses in HaCaT cells are mediated by the PI3-K/Akt pathway.
- S1P may be of use in a number of clinical conditions, including promotion of wound healing.

References

1 Hla T. Physiological and pathological actions of sphingosine 1-phosphate. *Semin Cell Dev Biol* 2004; **15**: 513–20.
2 Vogler R, Sauer B, Kim DS *et al.* Sphingosine-1-phosphate and its potentially paradoxical effects on critical parameters of cutaneous wound healing. *J Invest Dermatol* 2003; **120**: 693–700.
3 Kim DS, Kim SY, Kleuser B *et al.* Sphingosine-1-phosphate inhibits human keratinocyte proliferation via Akt/protein kinase B inactivation. *Cell Signal* 2004; **16**: 89–95.
4 Amano S, Akutsu N, Ogura Y *et al.* Increase of laminin 5 synthesis in human keratinocytes by acute wound fluid, inflammatory cytokines and growth factors, and lysophospholipids. *Br J Dermatol* 2004; **151**: 961–70.
5 Hammer S, Sauer B, Spika I *et al.* Glucocorticoids mediate differential anti-apoptotic effects in human fibroblasts and keratinocytes via sphingosine-1-phosphate formation. *J Cell Biochem* 2004; **91**: 840–51.
6 Manggau M, Kim DS, Ruwisch L *et al.* 1-Alpha,25-dihydroxyvitamin D3 protects human keratinocytes from apoptosis by the formation of sphingosine-1-phosphate. *J Invest Dermatol* 2001; **117**: 1241–9.
7 Uchida Y, Houben E, Park K *et al.* Hydrolytic pathway protects against ceramide-induced apoptosis in keratinocytes exposed to UVB. *J Invest Dermatol* 2010; **130**: 2472–80.
8 Roy S, Khanna S, Nallu K *et al.* Dermal wound healing is subject to redox control. *Mol Ther* 2006; **13**: 211–20.
9 Soneja A, Drews M, Malinski T. Role of nitric oxide, nitroxidative and oxidative stress in wound healing. *Pharmacol Report* 2005; **57**: 108–19.
10 Moriue T, Igarashi J, Yoneda K *et al.* Sphingosine 1-phosphate attenuates H2O2-induced apoptosis in endothelial cells. *Biochem Biophys Res Commun* 2008; **368**: 852–7.
11 Schuppel M, Kurschner U, Kleuser U *et al.* Sphingosine 1-phosphate restrains insulin-mediated keratinocyte proliferation via inhibition of Akt through the S1P2 receptor subtype. *J Invest Dermatol* 2008; **128**: 1747–56.
12 Boukamp P, Petrussevska RT, Breitkreutz D *et al.* Normal keratinization in a spontaneously immortalized aneuploid human keratinocyte cell line. *J Cell Biol* 1988; **106**: 761–71.
13 Yoneda K, Demitsu T, Nakai K *et al.* Activation of vascular endothelial growth factor receptor 2 in a cellular model of loricrin keratoderma. *J Biol Chem* 2010; **285**: 16184–94.
14 Igarashi J, Miyoshi M, Hashimoto T *et al.* Hydrogen peroxide induces S1P1 receptors and sensitizes vascular endothelial cells to sphingosine 1-phosphate, a platelet-derived lipid mediator. *Am J Physiol Cell Physiol* 2007; **292**: C740–8.
15 Shimizu H, Banno Y, Sumi N *et al.* Activation of p38 mitogen-activated protein kinase and caspases in UVB-induced apoptosis of human keratinocyte HaCaT cells. *J Invest Dermatol* 1999; **112**: 769–74.
16 Lewis DA, Hengeltraub SF, Gao FC *et al.* Aberrant NF-kappaB activity in HaCaT cells alters their response to UVB signaling. *J Invest Dermatol* 2006; **126**: 1885–92.
17 Chun J, Hartung HP. Mechanism of action of oral fingolimod (FTY720) in multiple sclerosis. *Clin Neuropharmacol* 2010; **33**: 91–101.
18 Sugita K, Kabashima K, Sakabe J *et al.* FTY720 regulates bone marrow egress of eosinophils and modulates late-phase skin reaction in mice. *Am J Pathol* 2010; **177**: 1881–7.
19 Bito T, Izu K, Tokura Y. Evaluation of toxicity and Stat3 activation induced by hydrogen peroxide exposure to the skin in healthy individuals. *J Dermatol Sci* 2010; **58**: 157–9.
20 Diker-Cohen T, Koren R, Ravid A. Programmed cell death of stressed keratinocytes and its inhibition by vitamin D. the role of death and survival signaling pathways. *Apoptosis* 2006; **11**: 519–34.
21 Yang B, Oo TN, Rizzo V. Lipid rafts mediate H_2O_2 prosurvival effects in cultured endothelial cells. *FASEB J* 2006; **20**: 1501–3.
22 Yatomi Y, Igarashi Y, Yang L *et al.* Sphingosine 1-phosphate, a bioactive sphingolipid abundantly stored in platelets, is a normal constituent of human plasma and serum. *J Biochem* 1997; **121**: 969–73.
23 Igarashi J, Bernier SG, Michel T. Sphingosine 1-phosphate and activation of endothelial nitric-oxide synthase. differential regulation of Akt and MAP kinase pathways by EDG and bradykinin receptors in vascular endothelial cells. *J Biol Chem* 2001; **276**: 12420–6.
24 Halin C, Scimone ML, Bonasio R *et al.* The S1P-analog FTY720 differentially modulates T-cell homing via HEV. T-cell-expressed S1P1 amplifies integrin activation in peripheral lymph nodes but not in Peyer patches. *Blood* 2005; **106**: 1314–22.
25 Kawanabe T, Kawakami T, Yatomi Y *et al.* Sphingosine 1-phosphate accelerates wound healing in diabetic mice. *J Dermatol Sci* 2007; **48**: 53–60.

Supporting Information

Additional Supporting Information may be found in the online version of this article:

Figure S1. Reverse transcription (RT)-PCR analysis of mRNA encoding S1P receptors in HaCaT cells.

Figure S2. FTY720-P pretreatment enhanced H_2O_2-induced phosphorylation of Akt in HaCaT cells.

Figure S3. FTY720-P pretreatment modulates H_2O_2-induced phosphorylation of signal transducer and activator of transcription (Stat)3 in HaCaT cells.
Figure S4. Pretreatment with higher dose of sphingosine 1-phosphate (S1P) did not attenuate H_2O_2-induced phosphorylation of Akt in HaCaT cells.
Figure S5. Sphingosine 1-phosphate (S1P) pretreatment attenuated the H_2O_2-induced cleavage of caspase-3 in HaCaT cells.
Table S1. Primers used for reverse transcription (RT)-PCR analysis.

THE JOURNAL OF DERMATOLOGY

doi: 10.1111/1346-8138.12360

Journal of Dermatology 2014; **41**: 1–2

LETTER TO THE EDITOR

Calcification of the placenta in a woman with pseudoxanthoma elasticum with a mutation of the *ABCC6* gene

Dear Editor,

A 26-year-old woman was referred to our department from an obstetrician at 12 weeks of gestation for evaluation of non-symptomatic yellowish papules on the neck and axillae, which appeared at the age of 20 years (Fig. 1a). Histological examination of a yellow papule on the right axilla showed a band of eosinophilic granular material in the dermis. Elastica van Gieson stain showed fragmentation and clumping of elastic

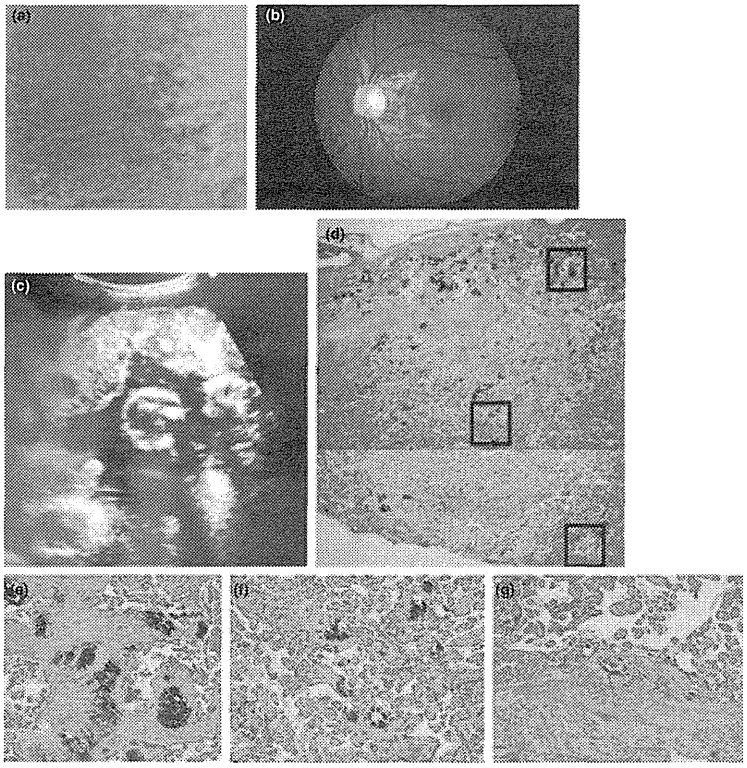

Figure 1. (a) Clinical presentation of yellow papules on the right axilla. (b) Fundus photograph of the patient's left eye. Whereas angioid streaks were observed around the optic disc and peau d'orange fundus was apparent temporal to the macula, no choroidal neovascularization was detected. (c) An echogram of the uterus at the 35th week detected calcification of the placenta. (d) Histological examination showed multiple calcified lesions in the placenta (hematoxylin–eosin [HE], ×12.5). The upper and lower parts were the fetal and maternal side of the placenta, respectively. (e) Calcification in chorion frondosum. High magnification of upper black box in (d) (fetal side) (HE, ×100). (f) Calcification in the villus. High magnification of middle black box in (d) (HE, ×100). (g) High magnification of the placenta in lower black box in (d) showed calcification of blood vessels in the decidua basalis (maternal side of the placenta) (HE, ×100).

Correspondence: Atsushi Utani, M.D., Ph.D., Department of Dermatology, Graduate School of Medicine, Nagasaki University, Nagasaki 606-8507, Japan. Email: utani@nagasaki-u.ac.jp

Author contribution: Drs Tanioka and Utani had full access to all of the data in the study and take responsibility for the integrity of the data and the accuracy of the data analysis. Study concept and design: Tamura, Kondo. Acquisition of data: Konishi, Yomisura. Analysis and interpretation of data: Utani, Tanioka, Kondo, Tamura. Drafting of the manuscript: Tanioka. Critical revision of the manuscript for important intellectual content: All authors. Statistical analysis: None. Administrative, technical, or material support: None. Study supervision: Miyachi, Konishi, Yoshimura.

Financial disclosure: None reported.

Approval: This study was approved by the local institutional review board.

fibers, where calcification of the degenerated fibrous components was revealed by von Kossa stain. Sequencing of the *ABCC6* gene detected a heterozygous mutation of C595T (nonsense mutation Q199X).

These skin lesions were diagnosed as pseudoxanthoma elasticum (PXE); thereafter, the other signs of PXE were screened by consulting specialists. Fundoscopic examination detected angioid streaks in both eyes, regardless of having no visual disturbance (Fig. 1b).

Electrocardiogram and echogram of the heart showed no abnormality and no calcification of large blood vessels.

At 30th week of pregnancy, a prenatal ultrasonography detected severe calcification of the placenta (Fig. 1c).

She delivered a healthy baby boy weighing 2810 g vaginally at the 39th week. The placenta (17 cm × 21 cm × 2.5 cm) weighed 640 g, and had grossly visible calcification. The calcification of vessels was evident not only in the decidua basalis (maternal side of the placenta) but also in the villus and the chorion frondosum (fetal side) (Fig. 1d–g). The umbilical arteries and vein showed slight blood congestion, but no calcification.

Pregnancy in PXE has been described to have severe complications, leading health-care providers to advise women with PXE against becoming pregnant. However, a study of 407 patients with PXE showed that it is not associated with markedly increased fetal loss or adverse reproductive outcomes.[1] On the other hand, a paper pointed out the risk on ocular lesions by labor and delivery.[2] Obstetric prognosis is dependent on the vascular damage caused by PXE. In the present case, screening examination could not find any vascular abnormalities.

The mechanism of calcification is speculated to be an abnormal function of calcium metabolism, because *ABCC6* is supposed to code a membrane transport protein.[3] Its substrate is still unknown, but is probably an organic anion, which prevents calcification in the body. We speculated that the putative factor, which prevents calcification, is missing in patients with PXE. Q199X is the second commonest mutation in Japanese patients with PXE. Ten out of 70 Japanese patients with PXE have this nonsense mutation.

Calcification is often found in the maternal side of the mature placenta even in women with non-PXE, while villous calcification is uncommon.[4] Calcification was much more pronounced in PXE than in controls in all placental regions; maternal side, villi and fetal side.[5] Also, in the present case, the calcification was more severe in the maternal side than in the fetal side.

The diagnosis of PXE is often difficult, however, skin lesions are the first indication of PXE, which usually appears during the first and second decade of life. Dermatological evaluation of a woman with severe calcification of the placenta may lead to a diagnosis of PXE.

CONFLICT OF INTEREST: None declared.

Miki TANIOKA,[1] Atsushi UTANI,[2] Hiroshi TAMURA,[3] Nagahisa YOSHIMURA,[3] Norihito KASHIWAGI,[4] Eiji KONDO,[5] Ikuo KONISHI,[5] Yoshiki MIYACHI[1]

[2]*Department of Dermatology, Nagasaki University Graduate School of Medicine, Nagasaki,* [1]*Departments of Dermatology,* [3]*Ophthalmology,* [4]*Department of Obstetrics and Gynecology, Kashiwagi Clinic, and* [5]*Obstetrics and Gynecology, Kyoto University Graduate School of Medicine, Kyoto, Japan*

REFERENCES

1 Bercovitch L, Leroux T, Terry S, Weinstock MA. Pregnancy and obstetrical outcomes in pseudoxanthoma elasticum. *Br J Dermatol* 2004; **151**: 1011–1018.
2 Farhi D, Descamps V, Picard C *et al.* Is pseudoxanthoma elasticum with severe angioid streaks an indication for Caesarean section? *J Eur Acad Dermatol Venereol* 2006; **20**: 1328–1399.
3 Li Q, Uitto J. Heritable ectopic mineralization disorders: the paradigm of pseudoxanthoma elasticum. *J Invest Dermatol* 2012; **132**: E15–E19.
4 Ramos-e-Silva M, Lı'bia Cardozo Pereir A, Oliveira G *et al.* Connective tissue diseases: pseudoxanthoma elasticum, anetoderma, and Ehlers-Danlos syndrome in pregnancy. *Clin Dermatol* 2006; **24**: 91–96.
5 Gheduzzi D, Taparelli F, Quaglino D *et al.* The placenta in pseudoxanthoma elasticum: clinical, structural and immunochemical study. *Placenta* 2001; **22**: 580–590.

ORIGINAL ARTICLE

An *Ex Vivo* Model Employing Keloid-Derived Cell–Seeded Collagen Sponges for Therapy Development

Yosuke Yagi[1,2,6], Eri Muroga[1,6], Motoko Naitoh[3], Zenzo Isogai[4], Seiya Matsui[1,5], Susumu Ikehara[2], Shigehiko Suzuki[3], Yoshiki Miyachi[1] and Atsushi Utani[2]

The most distinctive feature of keloid is the extreme deposition of extracellular matrix, including collagens and proteoglycans (PGs). The focus of this study was the PG versican, which presumably defines keloid volume because of its ability to retain large amounts of water through its component glycosaminoglycans (GAGs). The excessive deposition of versican in keloids was examined by immunohistochemical analysis and by upregulation of the versican gene in these lesions by real-time PCR. The latter showed that mesenchymal cells derived from keloid lesion (KL) cells continue to exhibit above-normal versican production in culture. To establish a model of GAG deposition in keloids, collagen sponges seeded with KL cells (KL-SPos) were implanted in the subcutaneous space of nude mice. After 1 month, the KL-SPos were significantly heavier than the fibroblast (Fb)-seeded sponges (Fb-SPos). This *ex vivo* model was subsequently used to examine an inhibitory ability of IL-1β that was identified to reduce versican *in vitro*. IL-1β or chondroitinase ABC, when injected directly, successfully reduced the weight of the KL-SPos. Thus, on the basis of the change in weight of the seeded sponges, this *ex vivo* model can be used to test therapies aimed at reducing or inhibiting keloid formation and to study the pathogenesis of this aberrant response.

Journal of Investigative Dermatology (2013) **133,** 386–393; doi:10.1038/jid.2012.314; published online 6 September 2012

INTRODUCTION

Keloids occur spontaneously or following minor trauma, expanding beyond the boundaries of the original wound and causing serious functional and cosmetic problems. In people predisposed to keloid development, normal wound-healing processes are derailed, leading to an exuberant cellular response that includes excessive extracellular matrix (ECM) production and deposition (Wolfram *et al.*, 2009).

Our group (Naitoh *et al.*, 2005), as well as others (Smith *et al.*, 2008), determined that ECMs are overexpressed in keloid tissues and cells, respectively, using microarray assays. Recently, we demonstrated that micro-RNA-mediated mechanisms, namely a significant decrease in the level of miR196, was involved in the increased collagen synthesis characteristic of keloids (Kashiyama *et al.*, 2012). In addition, we showed that in these lesions, elastic fiber formation is disrupted because of the excess amounts of the glycosaminoglycan (GAG), chondroitin sulfate (CS), and dermatan sulfate (DS) (Ikeda *et al.*, 2009).

Versican is a member of the CS/DS–proteoglycan (PG) family. It is distributed in a variety of soft tissues and participates in cell adhesion, migration, proliferation, differentiation, and cartilage development (Wu *et al.*, 2005; Matsumoto *et al.*, 2006).

The sulfate or carbonyl moieties that form the long GAG side chains of versican enable it to hold large amounts of water. As excessive PG deposition contributes significantly to keloid volume, the elimination of these molecules by targeted treatment would significantly contribute to resolving the clinical problems associated with keloid development. Currently, international clinical recommendations on scar management, including keloids, comprise several treatment modalities (Mustoe *et al.*, 2002). However, among these, triamcinolone, surgery, radiation, and combination therapy have been shown to actually promote the recurrence of keloids rather than permanently eliminate them (Al-Attar *et al.*, 2006; van de Kar *et al.*, 2007; Butler *et al.*, 2008). The difficulty in developing a successful therapeutic strategy is further complicated by the absence of an appropriate model of keloids, a refractory disorder that is specific to humans.

The GAG deposition model of keloids developed in this study was based upon our observation of increased versican

[1]*Department of Dermatology, Graduate School of Medicine, Kyoto University, Kyoto, Japan;* [2]*Department of Dermatology, Graduate School of Medicine, Nagasaki University, Nagasaki, Japan;* [3]*Plastic Reconstructive Surgery, Graduate School of Medicine, Kyoto University, Kyoto, Japan;* [4]*Department of Dermatology, National Center for Geriatrics and Gerontology, Aichi, Japan and* [5]*Drug Discovery Research Laboratories, Maruho Co., Ltd., Kyoto, Japan*

[6]*These authors contributed equally to this work.*

Correspondence: Atsushi Utani, Department of Dermatology, Graduate School of Medicine, Nagasaki University, 1-7-1 Sakamoto, Nagasaki 852-8501, Japan. E-mail: utani@nagasaki-u.ac.jp

Abbreviations: CS, chondroitin sulfate; DS, dermatan sulfate; ECM, extracellular matrix; Fb, fibroblast; GAG, glycosaminoglycan; KL, keloid lesion; PG, proteoglycan; RT-PCR, real-time PCR

Received 8 March 2012; revised 20 June 2012; accepted 9 July 2012; published online 6 September 2012

transcription in primary cultured keloid cells, as determined in promoter assays. Sponges seeded with these aberrant cells were implanted into the subcutaneous space of nude mice and were used to study the inhibitory effect of several compounds. Of the cytokines and growth factors tested, only IL-1β inhibited versican expression. Thus, this animal model provides an invaluable approach to the development of effective therapies aimed at reducing keloid formation, which can then be tested in human trials. Furthermore, it can be used to identify the *in vivo* components that promote ECM formation in these abnormal tissues.

RESULTS

Versican accumulation and upregulation of the gene in keloids

In a previous study (Ikeda *et al.*, 2009), we found that the ECM deposited in keloids contains large amount of CS and DS. Microarray assays analyzing these tissues showed that versican and other PGs comprising the ECM were expressed at higher levels than in nonlesional skin (Naitoh *et al.*, 2005). To confirm that versican is expressed at aberrantly high levels in keloids, we subjected six samples of keloids (K1–K6) to histopathological analysis. Hematoxylin–eosin staining revealed numerous fibrillar collagenous matrices forming a whorled pattern and a central collection of broad, compact, hyalinized, and collagenous bundles (Figure 1a). The presence of massive amounts of GAGs in these matrices was evidenced by toluidine blue staining (Figure 1a). Immunohistochemical analysis with anti-versican antibody demonstrated intense versican deposition in the keloids, but not in nonlesional skin (Figure 1a). However, there was no difference in hyaluronan accumulation (Figure 1a). These observations suggest that versican is a specific marker of keloids.

Alternative splicing produces several versican isoforms, designated V0–V3 (Wu *et al.*, 2005). Two major versican transcripts, namely the V0 and V1 isoforms, were detected in both normal human skin and in keloids by real-time PCR (RT-PCR) analysis (data not shown). RT-PCR analysis of the three keloid-derived RNAs and the three normal skin-derived RNAs revealed substantially higher versican mRNA levels in keloids than in normal skin (Figure 1b). Semiquantitative RT-PCR of the six keloid-derived RNAs (K1–K6) and the RNAs derived from five normal skin samples (N1–N5) showed a similar tendency (data not shown).

Primary cultured cells derived from keloids continue to overexpress PGs

Eight keloid cell lines (keloid lesion (KL) cells) were established from eight individuals and eight normal fibroblast (Fb) lines were established from another eight. Microarray analysis of the ECM using KL and Fb cell line showed that the former continued to overexpress ECM, and showed upregulation of three PGs (versican, aggrecan, and lumican) under the

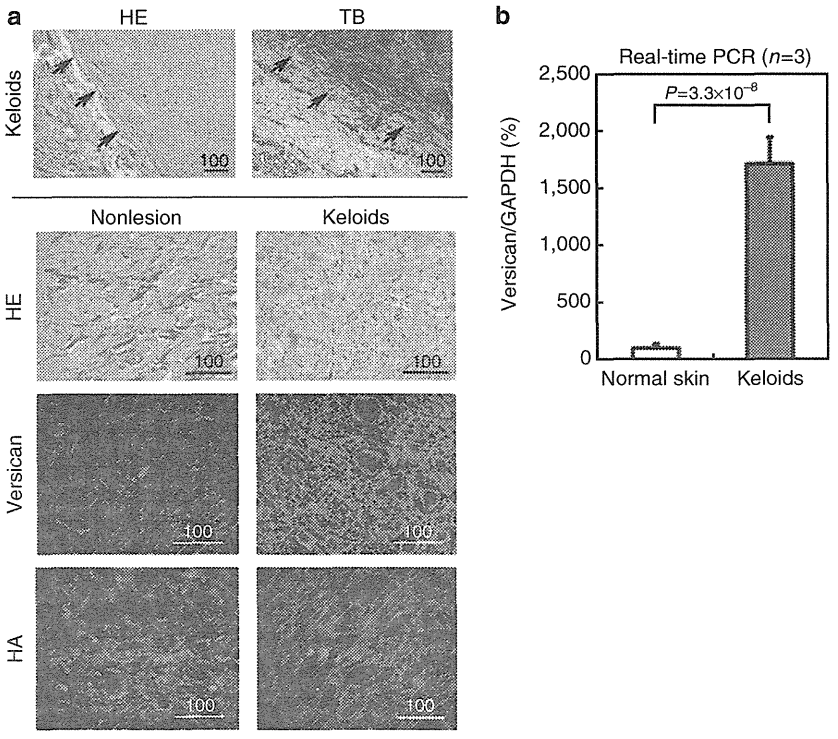

Figure 1. Versican accumulation and upregulation in keloids. (**a**) Hematoxylin–eosin (HE) staining revealed the deposition of an abnormal fibrillar collagenous matrix within the keloids. Toluidine blue (TB) staining at pH 2.5 showed metachromasia, indicative of glycosaminoglycan accumulation in the keloids. Arrows point to the boundary of the lesion. The keloids contained large deposits of versican, but there was no increase in hyaluronan (HA) levels. Representative images of the keloids obtained from six individuals are shown. Bar = μm. (**b**) Real-time PCR analysis of versican mRNA expression in samples of normal skin and of keloids. Mean ± SD and versican/glyceraldehyde 3-phosphate dehydrogenase ratios are shown.

Table 1. Microarray analysis of upregulated ECM genes in KL cells

Gene	Protein	mRNA KL cells /mRNA Fb[1]
COL10A1	Collagen α1 (X)	10.4
COL2A1	Collagen α1 (II)	10.3
ACAN	Aggrecan	6.2
COL9A1	Collagen α2 (IX)	3.9
COL11A1	Collagen α1 (XI)	3.6
LUM	Lumican	3.4
COL8A1	Collagen α1 (VIII)	2.8
VCAN	Versican	2.5
THBS1	Thrombospondin 1	2.4
COL17A1	Collagen α1 (XVII)	2.2
COL9A3	Collagen α3 (IX)	2.1

Abbreviations: ECM, extracellular matrix; Fb, fibroblast; KL, keloid lesion.
[1]Determined by microarray analysis performed in the current study.

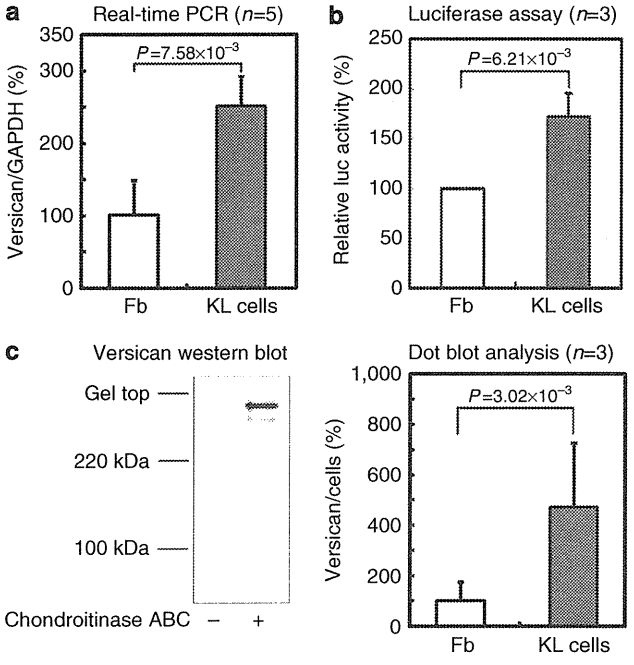

Figure 2. Versican upregulation in cultured keloid lesion (KL) cells. (**a**) KL cells and fibroblasts (Fbs) were analyzed for versican expression by real-time PCR. Versican/glyceraldehyde 3-phosphate dehydrogenase (GAPDH) ratios were calculated by setting the versican mRNA expression of one Fb cell line at 100%. The mean ± SD and the versican/GAPDH ratios are shown. (**b**) Both cells were transfected with a versican promoter luciferase reporter construct containing the versican promoter region (−559 to +353) and part of exon 1 fused to the luciferase gene. Luciferase activity was measured in quadruplicate and was calculated by setting the luciferase activity of one Fb cell line at 100%. Shown are the mean luciferase activities ± SD. (**c**) The antibody 2B1 specifically bound to versican (around 450 kDa). Dot-blot analysis of versican protein in conditioned medium.

culture conditions used (Table 1); all three PGs are upregulated in tissues (Naitoh *et al.*, 2005).

Upregulation of versican expression in KL cells

To determine whether versican is specifically upregulated in primary cultured KL cells, versican mRNA levels were measured. As shown by RT-PCR, the ratio of versican to glyceraldehyde 3-phosphate dehydrogenase expression in KL cells was 2.54 ± 0.53-fold higher than that in Fbs ($n = 5$ for both KL cells and Fbs) (Figure 2a). Furthermore, we used luciferase reporter assays to examine the activity of the versican promoter region, spanning −559 to +353, in KL cells and Fbs. As shown in Figure 2b, luciferase activity was 1.73 ± 0.22-fold higher in KL cells. After confirming that antibody 2B1 specifically bound to versican, we performed dot-blot analysis, which showed that KL cells overproduce versican protein (4.71 ± 2.53-fold higher than Fbs; Figure 2c).

Regulation of versican expression

Hypothesizing that a decrease in versican expression would lead to a corresponding reduction in keloid volume, we screened various cytokines, growth factors, and signaling pathway inhibitors. We carried out a series of studies in which LY294002, SB202190, and PD98059 were used to inhibit the PI3K, p38 MAPK, and ERK pathways, respectively. The results showed that PI3K and p38 MAPK, but not ERK, stimulated versican expression in both KL cells and Fbs (Figure 3a).

Among the growth factors and cytokines tested. The addition of IL-1β to Fbs and KL cells reduced versican expression in both, by 49.6 ± 13% and 21.2 ± 3.3%, respectively, compared with the corresponding untreated cells (Figure 3b). These results are consistent with other studies in which IL-1β reportedly suppressed versican expression in gingival Fbs (Qwarnstrom *et al.*, 1993) and arterial smooth muscle cells (Lemire *et al.*, 2007). Exogenous IL-1β also suppressed relative promoter activity in Fbs and KL cells, as evidenced by a decrease in luciferase activity of 65.8 ± 6.9% and 36.5 ± 10%, respectively (Figure 3c).

We then examined whether differences in the expression of IL-1β and IL-1 receptors by KL cells and Fbs accounted for the differential response to IL-1β and thus for the upregulation of versican in KL cells. ELISA assays showed that the amounts of endogenous IL-1β protein in the conditioned medium of both cell types were below the detectable limit (data not shown). Furthermore, according to RT-PCR, KL cells and Fb contain similar levels of IL-1 receptor mRNA (data not shown). Finally, the addition of an IL-1 receptor antagonist did not affect versican expression, although it completely blocked IL-1β-induced versican downregulation (Figure 3d). These results indicate that endogenous IL-1β is not involved in versican gene regulation under these experimental conditions.

Generation of an *ex vivo* GAG deposition model in mice

As noted above, keloid formation occurs only in humans, and thus there is no appropriate animal model. We therefore sought to establish an *ex vivo* model using the ECM-overproducing KL cells. In a previous study, we found that

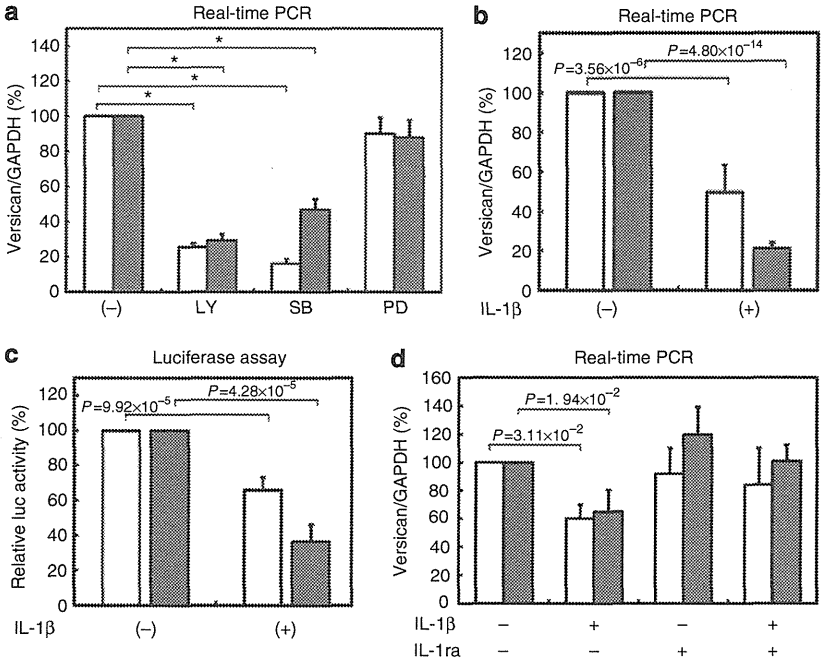

Figure 3. Analysis of signaling pathways and the effects of IL-1β on versican expression *in vitro*. (**a**) In keloid lesion (KL) cells (closed column) and fibroblasts (Fbs) (blank column), PI3K was blocked by the addition of LY294002 (LY), p38 MAPK by SB202190 (SB), and ERK by PD98059 (PD). *$P<0.001$. (**b**) KL cells or Fbs were treated with IL-1β. (**c**) Transfection was carried out 48 hours before stimulation of the cells with IL-1β (20 U ml^{-1}). (**d**) Both cell types were treated with recombinant IL-1 receptor antagonist and/or IL-1β. Versican/glyceraldehyde 3-phosphate dehydrogenase (GAPDH) ratios or luciferase promoter activity was calculated by setting the value obtained from the untreated KL cells or Fb at 100%. All experiments were performed in triplicate. Representative data, expressed as the mean ± SD, are shown.

cartilage could be successfully reconstructed using a collagen sponge as a scaffold for chondroprogenitor cells (Togo *et al.*, 2006). Accordingly, these sponges, which consist of chemically cross-linked collagen resistant to collagenase digestion *in vivo*, were used in our *ex vivo* model. Collagen sponges were seeded with 5×10^5 KL cells (KL-SPos) or Fbs (Fb-SPos) and then implanted into the subcutaneous space of nude mice (Figure 4a). After various incubation periods, the KL-SPo and Fb-SPo were removed and weighed. After 1 month, the KL-SPos were less translucent (Figure 4a) and were significantly heavier than the Fb-SPos (29 ± 8.1 mg vs 17 ± 6.9 mg, respectively; Figure 4a). In contrast, a 3D *in vitro* incubation of KL-SPos and Fb-SPos for 1 month did not result in significant weight differences (Figure 4b). In sponges incubated subcutaneously for 1 month, hematoxylin–eosin and alcian blue staining, respectively, showed that greater amounts of ground substances and GAGs had been deposited in the KL-SPos than in the Fb-SPos (Figure 4c). Immunostaining evidenced larger amounts of versican, but not of hyaluronan (data not shown), in the KL-SPos than in the Fb-SPos (Figure 4d).

Injections with chondroitinase ABC or IL-1β reduced implant growth

The implants were treated with chondroitinase ABC to determine whether the weight increase in the KL-SPo could be suppressed by removing the CS/DS chains of PGs, including versican. Weekly injections of 0.5 U of chondroitinase ABC for 1 month caused a significant reduction in the weight of KL-SPo (from 26 ± 6.7 mg to 14 ± 6.8 mg; Figure 5a). In the KL-SPos, alcian blue staining revealed that the chondroitinase ABC injections had substantially reduced GAG deposition (Figure 5b), whereas versican immunostaining demonstrated that the enzymatic removal of the CS/DS chains caused a significant decrease in the levels of the core proteins of the PGs (Figure 5b). These data suggest that versican deposition in the KL-SPos is mediated by CS/DS–chain interactions with other matrix components. In contrast, the amount of collagen deposition in the injected KL-SPos and uninjected KL-SPos was essentially the same, as shown by Masson trichrome staining (Figure 5b).

As exogenous IL-1β reduced versican expression *in vitro*, we tested its effect on KL-SPos. Although there were no significant differences in alcian blue staining, Masson trichrome staining, and versican immunostaining between IL-1β-treated and nontreated sponges (data not shown), a significant reduction of weight was achieved with three-times-weekly injections of the cytokine (Figure 5c).

DISCUSSION

Although it is clear that normal wound-healing processes are derailed in individuals predisposed to developing keloids, the pathogenic mechanisms of keloids are poorly understood, including those resulting in excess ECM production (Wolfram *et al.*, 2009). PGs are expressed in large amounts in keloids

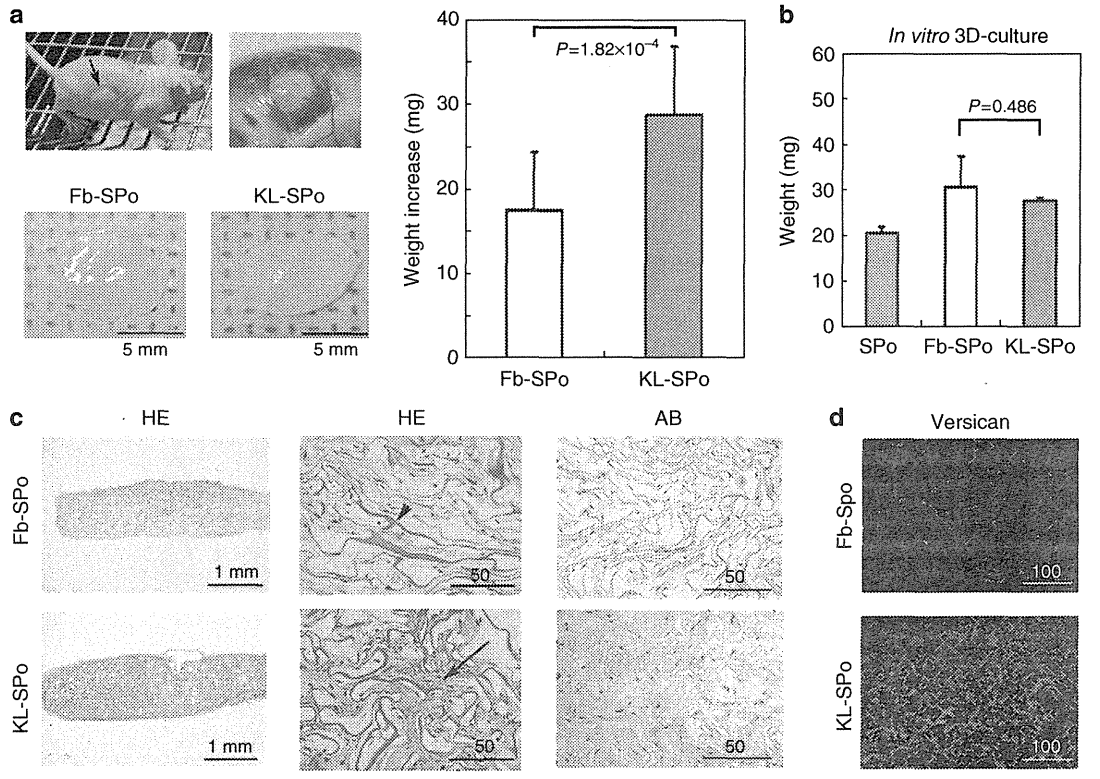

Figure 4. Generation of an *ex vivo* glycosaminoglycan deposition model in nude mice. (**a**) Collagen sponges seeded with keloid lesion (KL) cells (KL-SPos) or fibroblasts (Fb) (Fb-SPos) were implanted into the subcutaneous space of the mice (upper two images). After 1 month, the sponges were removed (lower two images). The mean ± SD of the increase in the weights of the sponges is shown. (**b**) SPo, Fb-SPo, and KL-SPo were cultured. The mean ± SD of the weights of samples is shown. (**c**) Sponges were stained with hematoxylin-eosin (HE), alcian blue (AB), and nuclear fast red. The arrowhead indicates the chemically cross-linked collagen fibers of the collagen sponges, and the arrow indicates the ground substance deposits. Bar = 1 or 50 μm. (**d**) Versican immunostaining of KL-SPos and Fb-SPos. Bar = 100 μm.

and, because of their GAG-mediated capacity to retain large amounts of water, are likely to have important roles in determining the volume of these aberrant tissues. We previously reported that the GAGs deposited in keloid tissues mainly consist of CS/DS (Ikeda *et al.*, 2009). Of the three PGs showing increased expression in keloids, lumican GAGs only carry keratan sulfate chains. Because the major GAG found in keloids is CS (Ikeda *et al.*, 2009), we ruled out lumican as one of the PGs whose level is increased in keloids. In our earlier study of keloids, we were unable to detect aggrecan expression by northern blotting; thus, we assumed its expressions to be weak in keloid tissue (Naitoh *et al.*, 2005). Therefore, we focused on versican as the major PG deposited in keloids.

Several groups have attempted to generate animal models of keloids (e.g., by implanting a piece of human keloid tissue into mice (Waki *et al.*, 1991; Polo *et al.*, 1998)); however, to date, they have not been widely used (Ramos *et al.*, 2008). Recently, hypertrophic scar tissue implanted into nude mice was shown to undergo a significant size reduction in response to the direct application of basic Fb growth factor (Eto *et al.*, 2012). However, we preliminarily tried to implant small pieces of keloid tissue into nude mice, but after 1 month, these pieces had undergone various degrees of size reduction, probably due to matrix degradation. It may be that size is a critical factor in the prolonged maintenance of the implanted tissue, which is influenced by the proper distribution of nutrients and/or oxygen from the surrounding tissue. In an earlier study, we succeeded in obtaining cartilage production in the subcutaneous space of nude mice by using a chemically cross-linked collagen sponge seeded with chondroprogenitor cells (Togo *et al.*, 2006). Accordingly, we speculated that these sponges would be an excellent material for studying the mechanisms of GAG deposition in keloids. Indeed, after 1 month, the KL-SPos were heavier than the Fb-SPos. This result in turn implied that the efficacy of test compounds in suppressing keloid volume could be estimated simply by weighing the sponges. Another advantage of the collagen sponges is that their elasticity facilitates injection with the various candidate therapeutic compounds. A sponge-like scaffold fabricated from polylactic acid (Chung *et al.*, 2008) was also tested, but it did not result in significant versican deposition (data not shown).

One of the aims of this study was to identify compounds that inhibited the growth of the KL-SPos. As TGF-β stimulates versican expression in dermal Fbs under *in vitro* conditions (Kahari *et al.*, 1991), blockade of the TGF-β signaling pathway may also be a potent candidate keloid-treatment modality. Similarly, it would be interesting to examine the

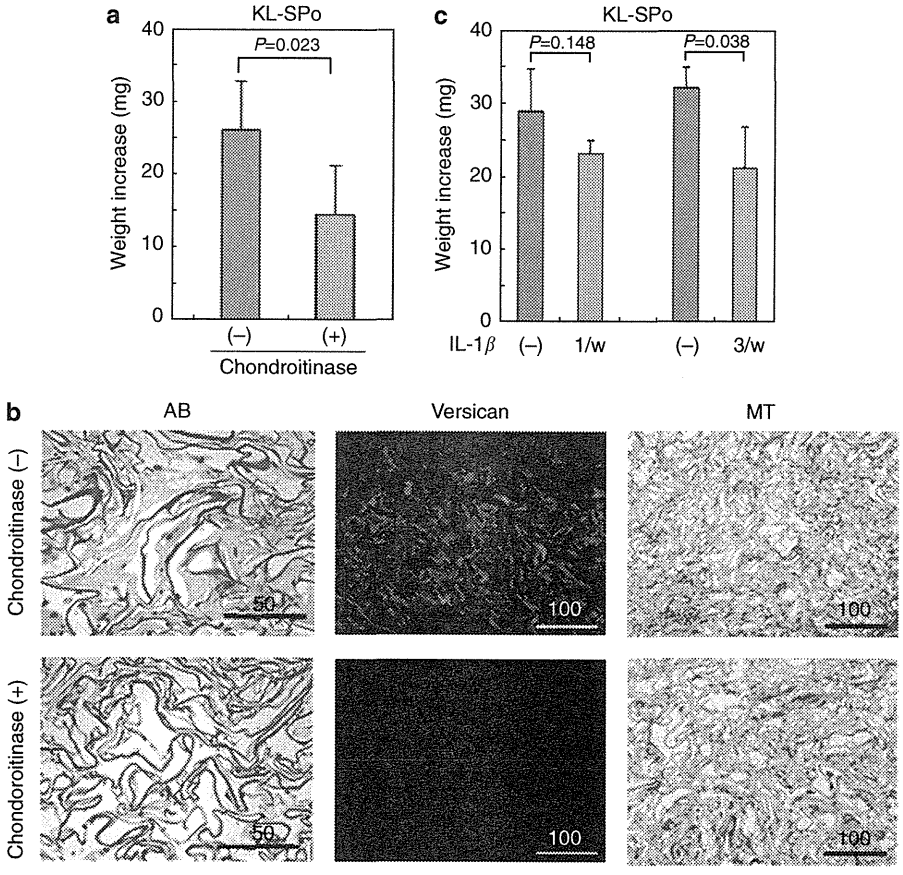

Figure 5. IL-1β injections reduce implant growth. (**a**) KL-SPos were transplanted into the subcutaneous space of nude mice. Chondroitinase ABC was injected into the sponges once a week for 1 month, starting 1 week post implantation. The sponges were then removed and immediately weighed. Shown are the mean ± SD implant weights of three animals per group (–): vehicle (0.1% BSA/H_2O). (**b**) Staining with alcian blue (AB) or Masson trichrome (MT), and immunostaining with anti-versican antibody of the chondroitinase ABC-treated (+) and -untreated (–) KL-SPos. Bar = μm. (**c**) IL-1β was injected into the sponges once or three times a week for 1 month, starting 1 week post implantation. Thrice-weekly injections significantly reduced the KL-SPo weight increase.

effects of PI3K and p38MAPK inhibitors on GAG deposition in our *ex vivo* system. Downregulation of versican deposition by IL-1β was observed in KL cells in our *ex vivo* model. Thus, IL-1β may be of therapeutic interest in keloids. Chondroitinase ABC may also be a potent inhibitor of keloid formation based on its ability to remove GAGs, as demonstrated in our *ex vivo* model. A reduction in keloid volume would be sufficient to relieve many of the clinical symptoms and cosmetic problems of affected individuals. Chondroitinase ABC is currently being tested in a phase III clinical trial in the USA and Japan for the treatment of interdisc herniation (http://www.seikagaku.co.jp/english/pdf/76.pdf). The results of that trial may be applicable to the treatment of keloids. Although there are currently several treatment modalities for keloids, many are unsatisfactory because they fail to prevent recurrence (Butler *et al.*, 2008). We developed a simple, reliable *ex vivo* model of keloids that can be used not only to evaluate novel anti-keloid agents but also to identify the mechanisms underlying the pathogenesis of keloids.

MATERIALS AND METHODS

Keloid samples and primary culture

Keloids are defined as raised, red, and inflexible scar tissue that invades the boundaries of the original wound (Butler *et al.*, 2008). Keloids and unaffected normal skin tissue specimens were obtained surgically with written informed consent, with adherence to the Declaration of Helsinki protocols, and with the approval of the Ethical Committee of the Kyoto University Medical School. Tissue samples were taken from keloids located on the shoulder, chest, or abdomen of six individuals (K1–K6, male:female ratio = 4:2; mean age = 36.3) and from normal skin tissue remaining after the surgical removal of benign tumors located on the face, buttock, abdomen, or inguinal region of five individuals (N1–N5, male:female ratio = 1:4; mean age = 31.6). All of the samples were subjected to histological examination and mRNA extraction.

Primary cultured cells were obtained from keloids located on the face, shoulder, chest, back, or abdomen of another eight individuals (male:female ratio = 6:2; mean age = 29.4) and from the normal skin of the face, forearm, buttock, or abdomen of eight additional individuals (male:female ratio = 5:3; mean age = 31.4). Primary cell

culture involved plating small pieces of excised keloid tissue on plastic dishes in 10% fetal bovine serum/DMEM with antibiotics and incubating the cultures at 37 °C until the cells grew out of the tissue pieces. These cells were maintained in the same culture medium and passaged by a 1:2–3 split when they reached early confluence.

For the signal inhibition assay, KL cells and Fbs were cultured in medium containing 30 μM LY294002 (PI3K inhibitor), 30 μM SB202190 (p38 MAPK inhibitor), or 20 μM PD98059 (ERK inhibitor; all from Calbiochem, Damstadt, Germany). For IL-1β signaling studies, the cells were cultured in the presence of IL-1β (20 U ml^{-1}; Roche Diagnostics, Indianapolis, IN). RNA was purified 15 hours after IL-1β treatment. Recombinant IL-1 receptor antagonist (0.5 μg ml^{-1}; R&D systems, Minneapolis, MN) was applied to both the KL cells and the Fbs 24 hours before RNA purification.

Animals and operations

The number of animals used in this study was kept to a minimum, and all possible efforts were made to reduce their suffering, in compliance with the protocols established by the Animal Research Committee of Kyoto University.

Immunohistochemistry

For versican immunostaining, mouse anti-human versican monoclonal antibody (2B1; from Seikagaku Kogyo, Tokyo, Japan) and Cy3-conjugated anti-mouse IgGs (Millipore-Chemicon, Billerica, MA) were used according to the manufacturer's instructions. For hyaluronan immunostaining, biotinylated hyaluronic acid-binding protein (Seikagaku Kogyo) and streptavidin-Cy3 (Sigma-Aldrich, St Louis, MO) were used according to the manufacturer's instructions. Fluorescence immunostaining was analyzed by confocal laser scanning microscopy using a Zeiss LSM 510 system (Carl Zeiss Microscopy, Göttingen, Germany).

RT-PCR

Total RNA was extracted and cDNA was synthesized as previously reported (Ikeda *et al.*, 2009). RT-PCR products were analyzed by quantitative RT-PCR by using TaqMan probe (Roche Applied Science, Mannheim, Germany), TaqMan Universal PCR Master Mix (Applied Biosystems, Carlsbad, CA), and the respective primers (Sigma-Aldrich) according to the manufacturer's instructions. Triplicate reactions were performed in an AB7300 real-time thermocycler (Applied Biosystems) under the following thermal cycles: 2 minutes at 50 °C, 1 minute at 95 °C, and 40 cycles of 15 seconds at 95 °C and 1 minute at 60 °C. The TaqMan probe and primers used were as follows: glyceraldehyde 3-phosphate dehydrogenase, probe no. 60, forward primer, (83–101 nt Genbank NM_002046.3) 5′-AGCCA CATCGCTCAGACAC-3′ and reverse primer (130–148 nt) 5′-GCCC AATACGACCAAATCC-3′; versican, probe no. 54, forward primer (9,657–9,675 nt Genbank NM_004385.3) 5′-GCACCTGTGTGCC AGGATA-3′ and reverse primer (9,703–9,726 nt) 5′-CAGGGATTA GAGTGACATTCATCA-3′; and IL-1 receptor, probe no. 60, forward primer (1,350–1,371 nt Genbank NM_000877.2) 5′-TGTTCATTTAT GGAAGGGATGA-3′ and reverse primer (1,403–1,427 nt) 5′-TTCTG CTTTTCTTTACGTTTTCATT-3′.

Transfection and luciferase assays

The promoter activity of KL cells and Fbs was assessed by inserting a −559 to +353 region of the human versican gene (GenBank U15963) (Naso *et al.*, 1994) upstream of the luciferase gene in the pTAL-luc plasmid (BD Biosciences Clontech, Palo Alto, CA). The construct was verified by DNA sequencing. KL cells or Fbs were seeded on 24-well plates at 1.5×10^5 cells per well and transfected with Fugene HD (Roche Applied Science) and their luciferase activities were measured with a Promega Dual Luciferase Reporter Assay kit (Promega, Madison, WI) according to the manufacturer's protocols.

Western and dot-blot analyses of versican protein

To collect conditioned medium, 2.0×10^5 KL cells or Fbs were seeded on six-well plates. Two days after serum starvation induced by culture in 2 ml of DMEM, conditioned medium was collected and used for western blot and dot-blot analyses, which were performed as described previously (Isogai *et al.*, 1996; Koyama *et al.*, 2007). Intensities of dots were calculated using ImageQuant TL (GE Healthcare, Amersham Place, UK). The values were expressed as the ratios to cell numbers.

Generation of an *ex vivo* GAG deposition model

Collagen sponges were prepared and were implanted into subcutaneous pockets of nude mice as previously reported (Togo *et al.*, 2006). Before implanting sponges, they were incubated overnight in 10% fetal bovine serum/DMEM with 5×10^5 KL cells or Fbs, thus generating KL-SPo and Fb-SPo, respectively. Four weeks after implantation, the KL-SPo and Fb-SPo were removed, weighed, and subjected to histological analysis as follows: after fixation with 10% phosphate-buffered formalin for 24 hours at 4 °C, the sponges were embedded in paraffin and sliced into 7.0-μm sections, which were either stained with hematoxylin–eosin or alcian blue (pH 2.5) or subjected to immunohistochemical analysis.

Injection of the collagen sponges with chondroitinase ABC and IL-1β

KL-SPos were injected once a week, starting 1 week post implantation, with *Proteus vulgaris* chondroitinase ABC (protease free: 0.1 U in 50 μl of 0.1% BSA/H_2O) or IL-1β (40 U in 20 μl of 0.1% BSA/phosphate-buffered saline). An equal amount of vehicle served as the control. At 4 weeks post implantation, the mice were killed and the sponges were removed and analyzed.

cDNA microarray analysis

Total RNA was isolated from cultured KL cells and Fbs using an RNeasy mini kit (Qiagen, Valencia, CA). Total RNA (1 μg) was amplified and labeled using the One-Cycle Target Labeling kit (Affymetrix, Santa Clara, CA).

Biotin-labeled cRNA (15 μg) was fragmented and hybridized to the GeneChip Human Genome U133 Plus 2.0 Array (Affymetrix). The array was incubated and signals were scanned according to the manufacturer's protocol. Expression profiles were analyzed based on the MAS5 algorithm using the GeneChip operating software (Affymetrix), with further analysis using GeneSpring 7.3 (Agilent Technologies, Palo Alto, CA). Raw intensity values from each chip were normalized to the 50th percentile of the measurements. Each gene was normalized to the median of that gene in the respective controls to enable the comparison of relative changes in gene expression levels between different conditions.

Statistical analysis

Student's *t*-test was used to examine differences between experimental groups. The data are expressed as the means ± SD. The calculated *P*-values were two-sided; $P<0.05$ was considered statistically significant.

CONFLICT OF INTEREST

The authors state no conflict of interest.

ACKNOWLEDGMENTS

We thank Dr Yoshihiko Yamada and Dr Kenneth Yamada, National Institute of Dental and Craniofacial Research, National Institutes of Health, for critical reading of the manuscript and their helpful suggestions. This work was supported in part by Grants-in-Aid (20591344 and 23659511) for Scientific Research from the Ministry of Education, Culture, Sports, Science and Technology of Japan, and by a grant from the Nakatomi Foundation to AU.

REFERENCES

Al-Attar A, Mess S, Thomassen JM *et al.* (2006) Keloid pathogenesis and treatment. *Plast Reconstr Surg* 117:286–300

Butler PD, Longaker MT, Yang GP (2008) Current progress in keloid research and treatment. *J Am Coll Surg* 206:731–41

Chung HJ, Steplewski A, Chung KY *et al.* (2008) Collagen fibril formation. A new target to limit fibrosis. *J Biol Chem* 283:25879–86

Eto H, Suga H, Aoi N *et al.* (2012) Therapeutic potential of fibroblast growth factor-2 for hypertrophic scars: upregulation of MMP-1 and HGF expression. *Lab Invest* 92:214–23

Ikeda M, Naitoh M, Kubota H *et al.* (2009) Elastic fiber assembly is disrupted by excessive accumulation of chondroitin sulfate in the human dermal fibrotic disease, keloid. *Biochem Biophys Res Commun* 390:1221–8

Isogai Z, Shinomura T, Yamakawa N *et al.* (1996) 2B1 antigen characteristically expressed on extracellular matrices of human malignant tumors is a large chondroitin sulfate proteoglycan, PG-M/versican. *Cancer Res* 56:3902–8

Kahari VM, Larjava H, Uitto J (1991) Differential regulation of extracellular matrix proteoglycan (PG) gene expression. Transforming growth factor-beta 1 up-regulates biglycan (PGI), and versican (large fibroblast PG) but down-regulates decorin (PGII) mRNA levels in human fibroblasts in culture. *J Biol Chem* 266:10608–15

Kashiyama K, Mitsutake N, Matsuse M *et al.* (2012) miR-196a downregulation increases the expression of type I and III collagens in keloid fibroblasts. *J Invest Dermatol* 132:1597–604

Koyama H, Hibi T, Isogai Z *et al.* (2007) Hyperproduction of hyaluronan in neu-induced mammary tumor accelerates angiogenesis through stromal cell recruitment: possible involvement of versican/PG-M. *Am J Pathol* 170:1086–99

Lemire JM, Chan CK, Bressler S *et al.* (2007) Interleukin-1 beta selectively decreases the synthesis of versican by arterial smooth muscle cells. *J Cell Biochem* 101:753–66

Matsumoto K, Kamiya N, Suwan K *et al.* (2006) Identification and characterization of versican/PG-M aggregates in cartilage. *J Biol Chem* 281:18257–63

Mustoe TA, Cooter RD, Gold MH *et al.* (2002) International clinical recommendations on scar management. *Plast Reconstr Surg* 110: 560–71

Naitoh M, Kubota H, Ikeda M *et al.* (2005) Gene expression in human keloids is altered from dermal to chondrocytic and osteogenic lineage. *Genes Cells* 10:1081–91

Naso MF, Zimmermann DR, Iozzo RV (1994) Characterization of the complete genomic structure of the human versican gene and functional analysis of its promoter. *J Biol Chem* 269:32999–3008

Polo M, Kim YJ, Kucukcelebi A *et al.* (1998) An *in vivo* model of human proliferative scar. *J Surg Res* 74:187–95

Qwarnstrom EE, Jarvelainen HT, Kinsella MG *et al.* (1993) Interleukin-1 beta regulation of fibroblast proteoglycan synthesis involves a decrease in versican steady-state mRNA levels. *Biochem J* 294(Part 2):613–20

Ramos ML, Gragnani A, Ferreira LM (2008) Is there an ideal animal model to study hypertrophic scarring? *J Burn Care Res* 29:363–8

Smith JC, Boone BE, Opalenik SR *et al.* (2008) Gene profiling of keloid fibroblasts shows altered expression in multiple fibrosis-associated pathways. *J Invest Dermatol* 128:1298–310

Togo T, Utani A, Naitoh M *et al.* (2006) Identification of cartilage progenitor cells in the adult ear perichondrium: utilization for cartilage reconstruction. *Lab Invest* 86:445–57

van de Kar AL, Kreulen M, van Zuijlen PP *et al.* (2007) The results of surgical excision and adjuvant irradiation for therapy-resistant keloids: a prospective clinical outcome study. *Plast Reconstr Surg* 119:2248–54

Waki EY, Crumley RL, Jakowatz JG (1991) Effects of pharmacologic agents on human keloids implanted in athymic mice. A pilot study. *Arch Otolaryngol Head Neck Surg* 117:1177–81

Wolfram D, Tzankov A, Pulzl P *et al.* (2009) Hypertrophic scars and keloids–a review of their pathophysiology, risk factors, and therapeutic management. *Dermatol Surg* 35:171–81

Wu YJ, La Pierre DP, Wu J *et al.* (2005) The interaction of versican with its binding partners. *Cell Res* 15:483–94

our data provide proof of concept support for targeting this molecule and its multi-cellular functions in psoriatic skin. Targeting VEGF topically may provide an effective new approach for treating mild-to-moderate psoriasis skin lesions by inhibiting angiogenesis and reducing leukocyte infiltration and KC proliferation.

Funding support

NLW is supported in part by grants from the National Institutes of Health (P30AR39750, P50AR05508, RO1AR063437; RO1AR062546) and the National Psoriasis Foundation.

Acknowledgments

The authors apologize to colleagues whose work could not be cited because of the space constraints. We thank Dr. John Rudge (Regeneron Pharmaceuticals, Tarrytown, NY) for providing VEGF-Trap and Dr. Thomas McCormick for feedback on the manuscript.

References

[1] Yancopoulos GD, Davis S, Gale NW, Rudge JS, Wiegand SJ, Holash J. Vascular-specific growth factors and blood vessel formation. Nature 2000;407:242–8.
[2] Kunstfeld R, Hirakawa S, Hong YK, Schacht V, Lange-Asschenfeldt B, Velasco P, et al. Induction of cutaneous delayed-type hypersensitivity reactions in VEGF-A transgenic mice results in chronic skin inflammation associated with persistent lymphatic hyperplasia. Blood 2004;104:1048–57.
[3] Jung K, Lee D, Lim HS, Lee S-I, Kim YJ, Lee GM, et al. Double anti-angiogenic and anti-inflammatory protein valpha targeting VEGF-A and TNF-alpha in retinopathy and psoriasis. J Biol Chem 2011;286:14410–18.
[4] Xia YP, Li B, Hylton D, Detmar M, Yancopoulos GD, Rudge JS. Transgenic delivery of VEGF to mouse skin leads to an inflammatory condition resembling human psoriasis. Blood 2003;102:161–8.
[5] Akman A, Yilmaz E, Mutlu H, Ozdogan M. Complete remission of psoriasis following bevacizumab therapy for colon cancer. Clin Exp Dermatol 2009;34:e202–4.
[6] Fournier C, Tisman G. Sorafenib-associated remission of psoriasis in hypernephroma: case report. Dermatol Online J 2010;16(17.).
[7] Wolfram JA, Diaconu D, Hatala DA, Rastegar J, Knutsen DA, Lowther A, et al. Keratinocyte but not endothelial cell specific overexpression of Tie2 leads to the development of psoriasis. Am J Pathol 2009;174:1443–58.
[8] Ward NL, Loyd CM, Wolfram JA, Diaconu D, Michaels CM, McCormick TS. Depletion of antigen-presenting cells by clodronate liposomes reverses the psoriatic skin phenotype in KC-Tie2 mice. Brit J Dermatol 2011;164:750–8.
[9] Schonthaler HB, Huggenberger R, Wculek SK, Detmar M, Wagner EF. Systemic anti-VEGF treatment strongly reduces skin inflammation in a mouse model of psoriasis. Proc Natl Acad Sci USA 2009;21264–69.

Doina Diaconu[a], Yi Fritz[a], Sean M. Dawes[a], Candace M. Loyd[a], Nicole L. Ward[a,b,*]
[a]*Department of Dermatology, Case Western Reserve University, Cleveland, OH 44106, USA;*
[b]*The Murdough Family Center for Psoriasis, University Hospitals Case Medical Center, Cleveland, OH 44106, USA*

*Corresponding author at: Case Western Reserve University, Department of Dermatology BRB519, 10900 Euclid Avenue, Cleveland, OH 44106, USA.
Tel.: +1 216 368 1111; fax: +1 216 368 0212
E-mail address: Nicole.ward@case.edu (N. Ward)

19 April 2013

http://dx.doi.org/10.1016/j.jdermsci.2013.08.005

Letter to the Editor

Co-existence of mutations in the *FBN1* gene and the *ABCC6* gene in a patient with Marfan syndrome associated with pseudoxanthoma elasticum

To the Editor,

Marfan's syndrome (MFS) is a disease with an autosomal dominant mode of inheritance that is manifested by characteristic skeletal abnormalities, including arachnodactyly, cardiovascular lesions (such as aortic dilatation), and ocular manifestations (such as ectopia lentis) [1]. The *FBN1* gene [2], which encodes fibrillin-1 (a component of elastic fibers), has been identified as the responsible gene. Pseudoxanthoma elasticum (PXE) is an autosomal recessive disorder that causes the ectopic mineralization of elastic fibers in soft connective tissues and mainly affects the eyes, skin, and cardiovascular system. The precise pathomechanisms of elastic fiber degeneration in PXE have not been fully elucidated despite a number of extensive studies [3]. The disease is linked to mutations in the ATP-binding cassette sub-family C member 6 (*ABCC6*) gene [4,5]. Here, we report the case of a patient who exhibited the clinical manifestations of both MFS and PXE and in whom pathological gene mutations were detected in both the *FBN1* gene and the *ABCC6* gene.

In 2003, a 64-year-old, tall Japanese woman presented with skin eruptions in her nuchal area, axillae, and groin. She had previously experienced angina pectoris and had undergone bypass surgery for coronary stenosis. The patient's family history revealed that her mother had been tall and had died of heart disease when the patient was a small child. A history and physical examination of her father revealed that he had no noteworthy clinical findings. The patient was the 5th of 5 siblings, and the eldest sister and the 4th sister had both been tall. The eldest sister had suddenly died of unknown causes in early childhood, and the 4th sister had died of aortic dissection. The patient had two children, a 38-year-old son and a 36-year-old daughter, and both had skeletal abnormalities that included a tall stature and arachnodactyly. Her son had undergone a Bentall operation for aortic dissection and aortic valve regurgitation as a child. Dermatological and ophthalmological examinations revealed no evidence of PXE in either child. The patient's family tree is shown in Fig. 1A.

At the time of the patient's initial examination, she was 165 cm tall and had an arm span of 185 cm. Dolichocephaly, pectus carinatum, disproportionately long limbs for her height, and arachnodactyly were noted (Fig. 1B). Numerous papules ranging in color from normal to yellow arrayed in a cobblestone pattern were observed in the nuchal area, axillae, and groin (Fig. 1C). Ophthalmological examinations revealed angioid streaks on her retinas. Radiography revealed linear calcifications in the upper limbs. The pathological findings for skin biopsy specimens from the affected sites consisted of clumps of fragmented basophilic fibers in the middle and lower layers of the dermis (Fig. 1D). Granular deposits that stained positive with von Kossa stain (Fig. 1E) were observed in specimens from the same sites.

A genomic DNA analysis of the patient's blood revealed a monoallelic nonsense mutation (c. 5454C > A: exon 44, p.Cys1818Stop) in the *FBN1* gene (Fig. 2A). Exon sequencing of *ABCC6* was performed using primers designed to eliminate *ABCC6* pseudogenes for exons 1–9 [6] and those designed by Prime 3 for